



Article

# Bacteriophages vB\_Sen-TO17 and vB\_Sen-E22, Newly Isolated Viruses from Chicken Feces, Specific for Several *Salmonella enterica* Strains

Katarzyna Kosznik-Kwaśnicka <sup>1</sup>, Łukasz Grabowski <sup>1</sup>, Michał Grabski <sup>2,3</sup>,  
Mateusz Kaszubski <sup>2</sup>, Marcin Górniak <sup>4</sup>, Agata Jurczak-Kurek <sup>4</sup>, Grzegorz Węgrzyn <sup>2</sup> and  
Alicja Węgrzyn <sup>1,\*</sup>

<sup>1</sup> Laboratory of Molecular Biology, Institute of Biochemistry and Biophysics, Polish Academy of Sciences, Kładki 24, 80-822 Gdansk, Poland; k.kwasnicka@hotmail.com (K.K.-K.); lukas.grabowski95@gmail.com (Ł.G.)

<sup>2</sup> Department of Molecular Biology, University of Gdansk, Wita Stwosza 59, 80-308 Gdansk, Poland; michal.grabski@phdstud.ug.edu.pl (M.G.); mateuszkaszubski5@wp.pl (M.K.); grzegorz.wegrzyn@biol.ug.edu.pl (G.W.)

<sup>3</sup> Institute of Oceanology, Polish Academy of Sciences, Powstańców Warszawy 55, 81-712 Sopot, Poland

<sup>4</sup> Department of Molecular Evolution, University of Gdansk, Wita Stwosza 59, 80-308 Gdansk, Poland; marcin.gorniak@ug.edu.pl (M.G.); agata.jurczak-kurek@ug.edu.pl (A.J.-K.)

\* Correspondence: alicja.wegrzyn@biol.ug.edu.pl; Tel.: +48-58-523-6024

Received: 28 October 2020; Accepted: 19 November 2020; Published: 21 November 2020



**Abstract:** Two newly discovered bacteriophages, isolated from chicken feces and infecting *Salmonella enterica* strains, are described in this report. These phages have been named vB\_Sen-TO17 and vB\_Sen-E22, and we present their molecular and functional characterization. Both studied viruses are able to infect several *S. enterica* strains and develop lytically, but their specific host ranges differ significantly. Electron microscopic analyses of virions have been performed, and full genome sequences were determined and characterized, along with molecular phylogenetic studies. Genomes of vB\_Sen-TO17 (ds DNA of 41,658 bp) and vB\_Sen-E22 (dsDNA of 108,987 bp) are devoid of homologs of any known or putative gene coding for toxins or any other proteins potentially deleterious for eukaryotic cells. Both phages adsorbed efficiently (>95% adsorbed virions) within 10 min at 42 °C (resembling chicken body temperature) on cells of most tested host strains. Kinetics of lytic development of vB\_Sen-TO17 and vB\_Sen-E22, determined in one-step growth experiments, indicated that development is complete within 30–40 min at 42 °C, whereas burst sizes vary from 9 to 79 progeny phages per cell for vB\_Sen-TO17 and from 18 to 64 for vB\_Sen-E22, depending on the host strain. Virions of both phages were relatively stable (from several percent to almost 100% survivability) under various conditions, including acidic and alkaline pH values (from 3 to 12), temperatures from –80 °C to 60 °C, 70% ethanol, chloroform, and 10% DMSO. These characteristics of vB\_Sen-TO17 and vB\_Sen-E22 indicate that these phages might be considered in further studies on phage therapy, particularly in attempts to eliminate *S. enterica* from chicken intestine.

**Keywords:** bacteriophages; *Salmonella*; lytic development; genomic analysis

## 1. Introduction

Among various foodborne pathogenic bacteria, *Salmonella enterica* is one of the major infection agents responsible for human diseases caused by contamination of poultry-derived products [1]. While this bacterium usually does not induce any disorders in birds, it can be dangerous to humans. Abundance of *S. enterica* in chicken gut may result in contamination of poultry-derived food appearing

during the production process [2]. There are various serotypes of *S. enterica* which can cause diseases in humans, and the problem of salmonellosis is global [3]. In many countries, detection of specific serotypes of *S. enterica* (in most cases Typhimurium and Enteritidis) in poultry is considered as a compulsion to liquidate the whole flock [1].

Eradication of *S. enterica* can be performed using antibiotics; however, this method has met serious and global problems [4]. Bacterial strains resistant to many antibiotics are already known, which causes real crisis in therapies of infectious diseases [5,6]. Therefore, it is clear that development of novel methods of treatment of diseases caused by bacteria is necessary [7,8]. Phage therapy, i.e., the use of bacteriophages to combat bacterial infections, is one of the possible options [9]. Nevertheless, development of this method is not simple and requires specific conditions [9–11]. It is necessary to establish collections of potentially useful phages which can kill bacteria by conducting lytic development. Since phages are usually very specific to their hosts, such collections should be large to give a possibility of finding viruses capable of propagation in a particular bacterial strain isolated from patients or infected animals. Such bacteriophages must not contain genes coding for toxins and other proteins that might cause damage of human or animal cells. Therefore, it is still necessary to isolate previously unknown bacteriophages and to characterize them [9–11].

The proposal of the use of phage therapy to treat *Salmonella* infections has been published previously in many reports. Those studies led to determination of properties of various *Salmonella*-specific phages [12–21], effects of application of phages to poultry [22–27], and results of experimental use of phages in therapies of infected animals [28–32]. In addition, economic analyses of potential use of anti-*Salmonella* phage therapy in poultry have also been published [1,33]. Despite promising results of these studies, it was also indicated that most phages infecting *S. enterica* have a relatively narrow host range, specific to one or a few serovars or strains [12–21,34]. Thus, characterization of newly isolated bacteriophages infecting this bacterium is reasonable. Following this line of studies, in this report we present isolation and characterization (at both molecular and functional levels) of newly discovered bacteriophages specific to several strains of *S. enterica*.

## 2. Results

### 2.1. Isolation of Bacteriophages

Newly discovered bacteriophages were isolated from homogenates of chicken feces, using *S. enterica* serovars Typhimurium 13 and Enteritidis 1392 as hosts, according to a method described in Section 4.3. We isolated 25 different phages which formed five different types of plaques: (i) Turbid with diameter < 1 mm, (ii) turbid with diameter > 1 mm, (iii) clear with diameter < 1 mm, (iv) clear with diameter > 1 mm, and (v) clear with diameter > 1 mm and forming a halo. Two phages were selected for further analysis—the first one isolated using *S. Typhimurium* 13 as a host (bacteriophage named vB\_Sen-TO17) and the second one isolated using *S. Enteritidis* 1392 as a host (bacteriophage named vB\_Sen-E22).

### 2.2. Plaque and Virion Morphologies

The first steps of characterization of newly isolated bacteriophages consisted in determination of morphologies of plaques formed by them and morphologies of virions. Both tested phages formed clear plaques on lawns of the *S. Typhimurium* 13 host; however, vB\_Sen-TO17 produced significantly larger plaques (with additional halo) than vB\_Sen-E22 (Figure 1 and Table 1).

Virion morphology was investigated using electron microscopic methods. Both vB\_Sen-TO17 and vB\_Sen-E22 are caudate bacteriophages. They have been classified to families *Siphoviridae* and *Demerecoviridae*, respectively, on the basis of morphology of virions and molecular phylogenetic analyses (see Section 2.7). Electron micrographs of virions of both investigated phages are demonstrated in Figure 2, and quantified details of head and tail structures of virions of vB\_Sen-TO17 and vB\_Sen-E22 are presented in Table 1.

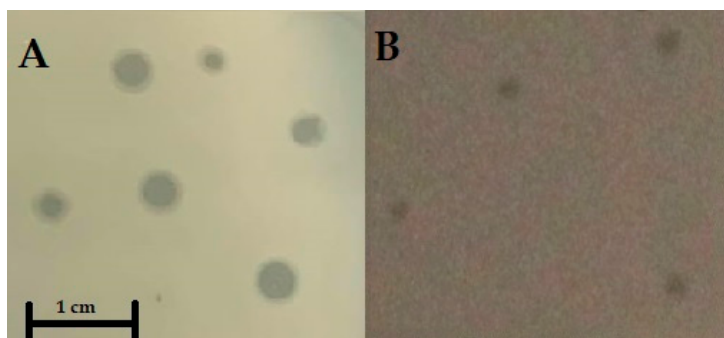


**Figure 1.** Morphology of plaques of vB\_Sen-TO17 (A) and vB\_Sen-E22 (B), formed on a lawn of the *S. Typhimurium* 13 host. A size bar (representing 1 cm) is shown at the bottom of panel A.

**Table 1.** Morphological characteristics of phages vB\_Sen-TO17 and vB\_Sen-E22. Experiments were performed using *S. Typhimurium* 13 as a host.

Phage Name	Plaque Morphology	Capsid Morphology		
		Head Diameter	Tail Length	Tail Width
vB_Sen-TO17	Clear, Ø 2.3–2.5 mm, with halo	48 ± 5 nm	121 ± 8 nm	10 ± 3 nm
vB_Sen-E22	Clear, Ø 0.8–1.0 mm	58 ± 3 nm	88 ± 6 nm	12 ± 2 nm

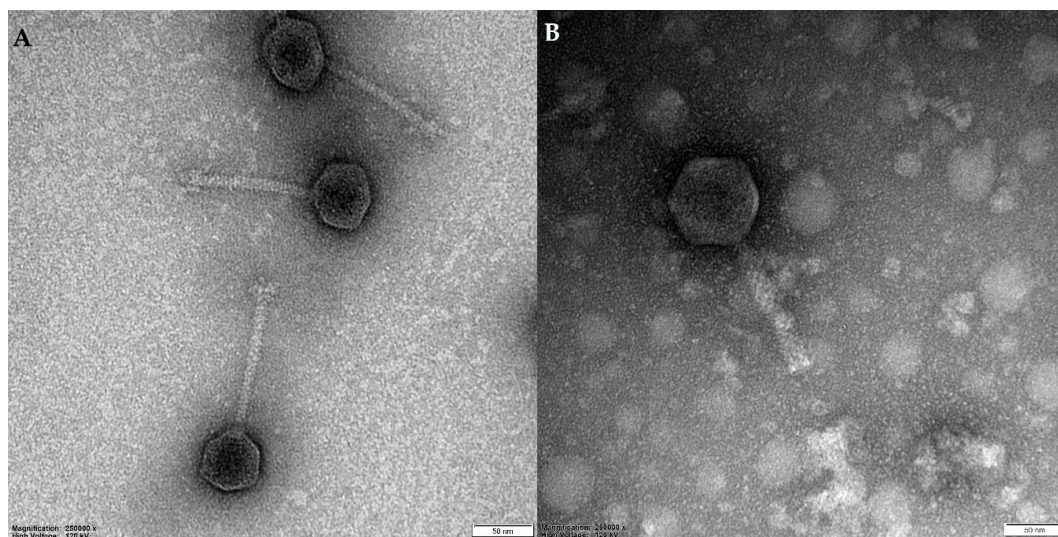


**Figure 2.** Electron micrographs of virions of vB\_Sen-TO17 (A) and vB\_Sen-E22 (B). Size bars (representing 50 nm) are shown at the bottom of each micrograph.

### 2.3. Host Range and Lysogenization Ability

Host ranges of vB\_Sen-TO17 and vB\_Sen-E22 were determined using various strains of *S. enterica*, representing different serovars. In control experiments, bacterial species either closely related to *S. enterica*, like *Escherichia coli*, or more distant were used. As expected, these experiments confirmed that vB\_Sen-TO17 and vB\_Sen-E22 are specific for *S. enterica*, while revealing different specificities to various strains, with vB\_Sen-E22 effectively infecting significantly more strains than vB\_Sen-TO17 (Table 2). Nevertheless, *S. enterica* Gallinarum 74 was infected by vB\_Sen-TO17 but not by vB\_Sen-E22. These results suggest that both investigated phages might be potentially useful in phage therapy.

**Table 2.** Host range of phages vB\_Sen-TO17 and vB\_Sen-E22.

Bacterial Strain	Efficiency of Plating (%) *	
	vB_Sen-TO17	vB_Sen-E22
<i>Citrobacter freundii</i>	<0.01	<0.01
<i>Enterococcus faecalis</i> 230	<0.01	<0.01
<i>Enterococcus faecalis</i> 243	<0.01	<0.01
<i>Escherichia coli</i> C600	<0.01	<0.01
<i>Escherichia coli</i> MG1655	<0.01	<0.01
<i>Lactobacillus acidophilus</i> 314 <sup>TM</sup>	<0.01	<0.01
<i>Lactococcus lactis</i> 49032 <sup>TM</sup>	<0.01	<0.01
<i>Proteus vulgaris</i>	<0.01	<0.01
<i>Salmonella enterica</i> Agona 1408	<0.01	<0.01
<i>Salmonella enterica</i> Bovismorbificans 300	<0.01	<0.01
<i>Salmonella enterica</i> Choleraesuis 1439	<0.01	<0.01
<i>Salmonella enterica</i> Choleraesuis 34	<0.01	68.49 ± 7.38
<i>Salmonella enterica</i> Choleraesuis var. Kunzendorf 37	<0.01	31.72 ± 2.55
<i>Salmonella enterica</i> Derby 20	<0.01	<0.01
<i>Salmonella enterica</i> Dublin 65	<0.01	85.94 ± 6.12
<i>Salmonella enterica</i> Enteritidis 1392	<0.01	100.00 ± 3.16
<i>Salmonella enterica</i> Enteritidis 64	39.27 ± 4.87	65.66 ± 5.18
<i>Salmonella enterica</i> Gallinarum 74	86.72 ± 4.55	<0.01
<i>Salmonella enterica</i> Hadar 1748	<0.01	<0.01
<i>Salmonella enterica</i> Heidelberg 16	<0.01	91.83 ± 6.82
<i>Salmonella enterica</i> Infantis 155	<0.01	<0.01
<i>Salmonella enterica</i> Kentucky 1368	<0.01	<0.01
<i>Salmonella enterica</i> Newport 50	<0.01	18.25 ± 6.51
<i>Salmonella enterica</i> Newport 51	<0.01	<0.01
<i>Salmonella enterica</i> Saintpaul 435	<0.01	<0.01
<i>Salmonella enterica</i> Senftenberg 87	<0.01	56.68 ± 4.39
<i>Salmonella enterica</i> Stanley 15	<0.01	8.48 ± 1.32
<i>Salmonella enterica</i> Thompson 39	<0.01	<0.01
<i>Salmonella enterica</i> Typhimurium 12	100.00 ± 3.22	97.88 ± 4.13
<i>Salmonella enterica</i> Typhimurium 13	100.00 ± 2.18	100.00 ± 6.43
<i>Salmonella enterica</i> Virchow 41	<0.01	85.42 ± 2.77
<i>Staphylococcus aureus</i> 6538 <sup>TM</sup>	<0.01	<0.01

\* Efficiency of plating was calculated on the basis of three independent experiments, and mean values ± SD are shown. Results obtained with *S. Typhimurium* 13 were considered as 100%, and other values reflect these results.

To test the ability of vB\_Sen-TO17 and vB\_Sen-E22 to lysogenize host cells, we performed efficiency of lysogenization assessment as described in Section 4.7. However, none of the tested phages were able to form prophages in 10 tested host strains, *S. Agona* 1408, *S. Dublin* 65, *S. Enteritidis* 64, *S. Enteritidis* 1392, *S. Heidelberg* 16, *S. Infantis* 155, *S. Newport* 50, *S. Typhimurium* 12, *S. Typhimurium* 13, and *S. Virchow* 41 (data not shown as no positive results of the test were observed).

#### 2.4. Sensitivity of Bacteriophages to Various Conditions

To test if vB\_Sen-TO17 and vB\_Sen-E22 are sensitive to different environmental conditions, we tested the survival of virions under various pH (focusing mostly on low pH conditions, which resemble those occurring in a stomach), the presence of various solvents, and the various temperatures of storage and lytic development.

As indicated in Table 3, while vB\_Sen-TO17 and vB\_Sen-E22 were completely inactivated at pH 2 or lower, significant fractions of viruses could survive in low pH conditions of 2.5 (about 4–8%) or 3.0 (about 55–67%). Moreover, these viruses could also survive in high pH conditions (about 72–85% at pH 10, and about 31–38% at pH 12). These phages were also relatively resistant to ethanol, chloroform, and DMSO, but not to acetone (Table 4). Large fractions (over 55% of virions) of vB\_Sen-TO17 and vB\_Sen-E22 could survive at temperatures between –80 °C and 60 °C, but not at 95 °C (Table 5). Optimal

temperatures for lytic development of both phages were between 37 °C and 42 °C, while vB\_Sen-E22 produced its progeny efficiently also at as low a temperature as 20 °C (Table 6). All these results indicate that vB\_Sen-TO17 and vB\_Sen-E22 are relatively resistant to various environmental conditions, suggesting their potential practical usefulness.

**Table 3.** Susceptibility of phages vB\_Sen-TO17 and vB\_Sen-E22 to different pH.

Phage Name	Phage Survivability in Studied Conditions (Relative Phage Titer in %)								
	pH 1.8	pH 2.0	pH 2.2	pH 2.5	pH 2.8	pH 3.0	pH 7.0 *	pH 10.0	pH 12.0
vB_Sen-TO17	<0.01	<0.01	11.11 ± 2.87	7.78 ± 2.21	18.89 ± 3.46	66.67 ± 7.15	100	85.41 ± 5.66	38.75 ± 3.89
vB_Sen-E22	<0.01	<0.01	<0.01	3.89 ± 0.95	33.33 ± 6.17	55.56 ± 8.55	100	72.43 ± 9.22	31.55 ± 4.72

Values obtained at pH 7.0 (marked as \*) were assessed as 100% and other values reflect these controls.

**Table 4.** Survivability of phages vB\_Sen-TO17 and vB\_Sen-E22 at different solvents, media, and buffers.

Phage Name	Phage Survivability in Studied Conditions (Relative Phage Titer in %)						
	70% Ethanol	Chloroform	90% Acetone	10% DMSO	DMEM	10% SDS	0.89% NaCl *
vB_Sen-TO17	42.63 ± 4.22	83.33 ± 5.37	0.88 ± 0.07	66.42 ± 7.15	100 ± 3.16	34.62 ± 7.16	100
vB_Sen-E22	8.75 ± 1.27	79.81 ± 6.42	0.23 ± 0.04	76.63 ± 6.85	100 ± 4.28	27.81 ± 4.21	100

Values obtained for 0.89% NaCl (marked as \*) were assessed as 100% and other values reflect these controls.

**Table 5.** Survivability of phages vB\_Sen-TO17 and vB\_Sen-E22 at different temperatures.

Phage Name	Phage Survivability at Different Temperatures (Relative Phage Titer in %)							
	−80 °C (24h)	−20 °C (24h)	4 °C (24h)	25 °C (24h)	37 °C * (1h)	42 °C (1h)	60 °C (1h)	95 °C (5min)
vB_Sen-TO17	86.26 ± 2.6	85.71 ± 2.25	85.70 ± 3.47	71.42 ± 4.66	100.00	61.94 ± 3.16	66.78 ± 2.8	<0.01
vB_Sen-E22	62.46 ± 4.8	55.56 ± 6.54	100.00 ± 2.81	100.00 ± 5.18	100.00	100.00 ± 2.75	88.88 ± 3.16	<0.01

Values obtained at 37 °C (marked as \*) were assessed as 100% and other values reflect these controls.

**Table 6.** Efficacy of phage plating of phages vB\_Sen-TO17 and vB\_Sen-E22 at different temperatures. Control temperature is marked with an asterisk.

Phage Name	Phage Propagation at Different Temperatures (Relative Phage Titer in %)			
	20 °C	25 °C	37 °C *	42 °C
vB_Sen-TO17	77.58 ± 2.66	83.78 ± 4.83	100.00	100.00 ± 6.21
vB_Sen-E22	100.00 ± 3.81	98.22 ± 4.77	100.00	100.00 ± 3.22

Values obtained at 37 °C (marked as \*) were assessed as 100% and other values reflect these controls.

### 2.5. Adsorption Efficiency and Kinetics of Lytic Development

We found that phages vB\_Sen-TO17 and vB\_Sen-E22 adsorbed efficiently on cells of various *S. enterica* strains, with above 95% efficiency within 10 min; the exception was the *S. Enteritidis* 64 host on which the adsorption efficiency was about 80% within 10 min (Figure 3). Therefore, this strain appears to be somewhat resistant to its recognition by virions during the first stages of development of phages vB\_Sen-TO17 and vB\_Sen-E22.

Kinetics of phage development have been investigated in one-step growth experiments. As both phages were isolated from chicken feces and were propagated on *S. enterica*, these experiments were performed at 42 °C to resemble conditions occurring in chicken intestine. While efficiency of lytic development was different in various host strains, the eclipse period was between 10 and 20 min, and the development was complete within 30–40 min (Figure 4). Burst sizes of Sen-TO17 and vB\_Sen-E22 varied between different host strains, ranging from 9 to 79 progeny phages per cell for vB\_Sen-TO17 and from 18 to 64 for vB\_Sen-E22 (Table 7). These results indicate that lytic development of both vB\_Sen-TO17 and vB\_Sen-E22 is effective in various *S. enterica* host strains at 42 °C.

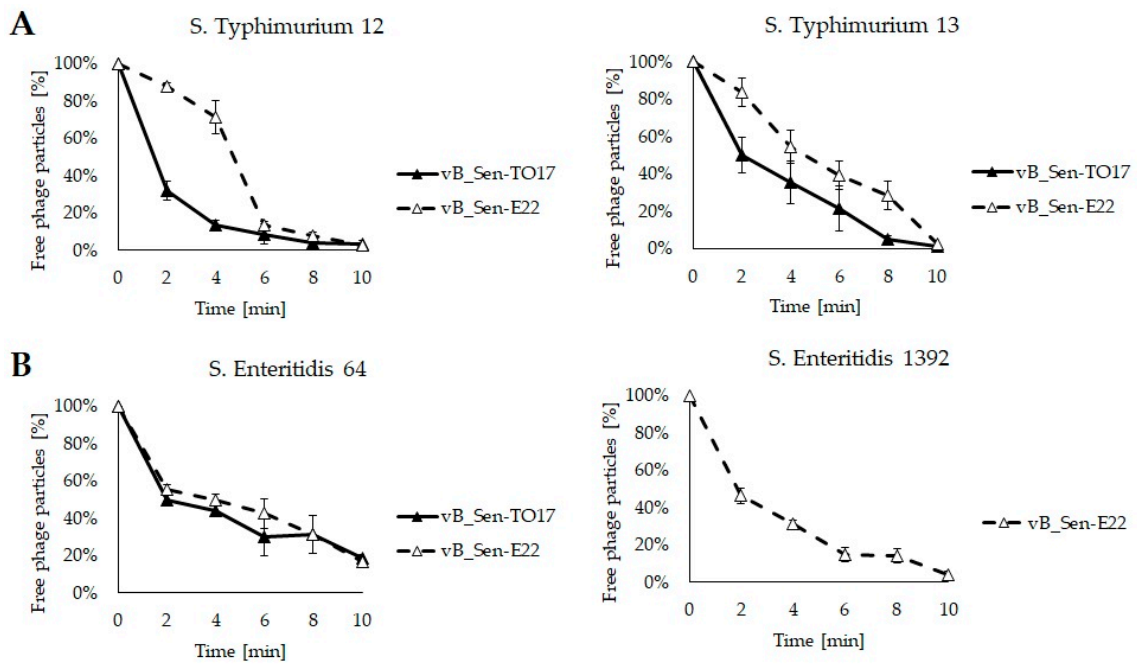


**Figure 3.** Adsorption rates of phages vB\_Sen-TO17 (closed triangles) and vB\_Sen-E22 (open triangles) on *S. Typhimurium* (A) and *S. Enteritidis* (B) at 42 °C. Number of free phage particles at time 0 was used as reference value (100%). Mean values from three independent experiments are shown, with error bars representing SD. Note that *S. Enteritidis* 1392 is resistant to vB\_Sen-TO17 (Table 2); thus, experiments with this strain were performed only for vB\_Sen-E22.

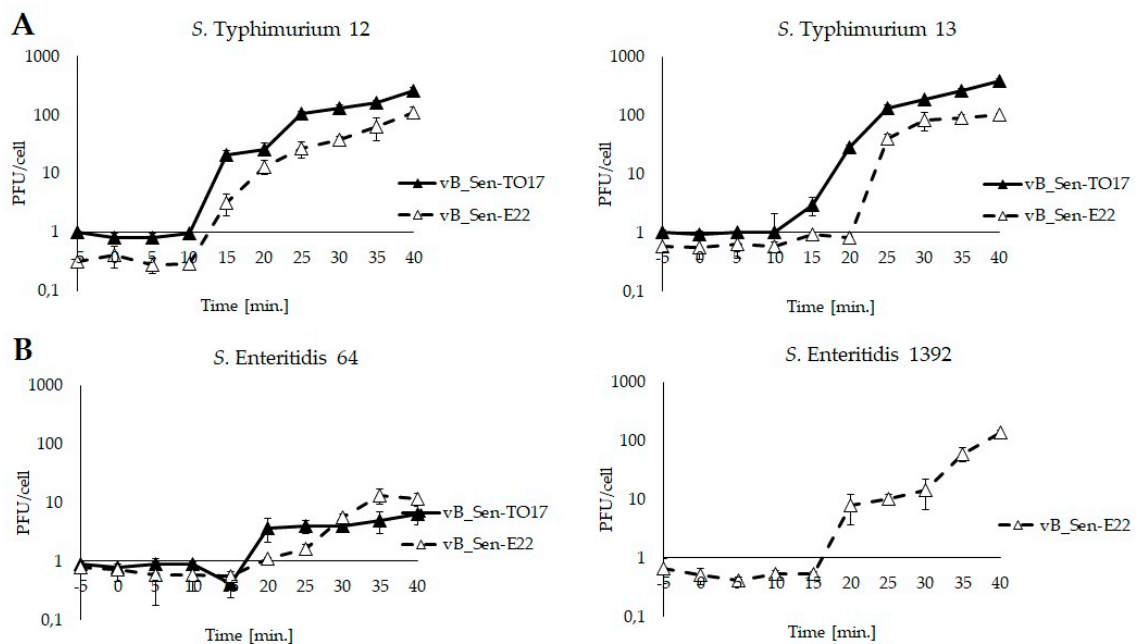


**Figure 4.** One-step growth experiments with phages vB\_Sen-TO17(closed triangles) and vB\_Sen-E22 (open triangles) on *S. Typhimurium* (A) and *S. Enteritidis* (B) at 42 °C; m.o.i. = 0.01. Mean values from three independent experiments are shown, with error bars representing SD. Note that *S. Enteritidis* 1392 is resistant to vB\_Sen-TO17 (Table 2); thus, experiments with this strain were performed only for vB\_Sen-E22.

**Table 7.** Burst size of phages vB\_Sen-TO17 and vB\_Sen-E22 on different *S. enterica* strains at 42 °C. The burst size was calculated from samples untreated with chloroform during the one-step growth experiment. Mean values from three independent experiments with SD are presented.

Phage Name	<i>Salmonella enterica</i> Strain		Burst Size (PFU/cell)
	Serotype	No.	
vB_Sen-TO17	Typhimurium	12	58.88 ± 4.71
		13	79.17 ± 3.77
	Enteritidis	64	9.27 ± 2.57
		1392	-
vB_Sen-E22	Typhimurium	12	55.48 ± 4.82
		13	64.83 ± 6.36
	Enteritidis	64	18.43 ± 2.15
		1392	57.74 ± 8.47

### 2.6. Analysis of Phage Genomes

DNA was isolated from purified virions of vB\_Sen-TO17 and vB\_Sen-E22 and subjected to sequencing, as described in Section 4.14. Annotations of vB\_Sen-TO17 and vB\_Sen-E22 genomes are presented in Tables S1 and S2, respectively.

The genome of phage vB\_Sen-TO17 (whole sequence deposited in GenBank; accession no. MT012729) consists of 41,658 bps, arranged in a linear topology with an overall GC content of 50.78% (Figure 5). We identified open reading frames (ORFs) putatively coding for 75 proteins, of which 27 were reported previously. The remaining 48 ORFs are described as hypothetical.

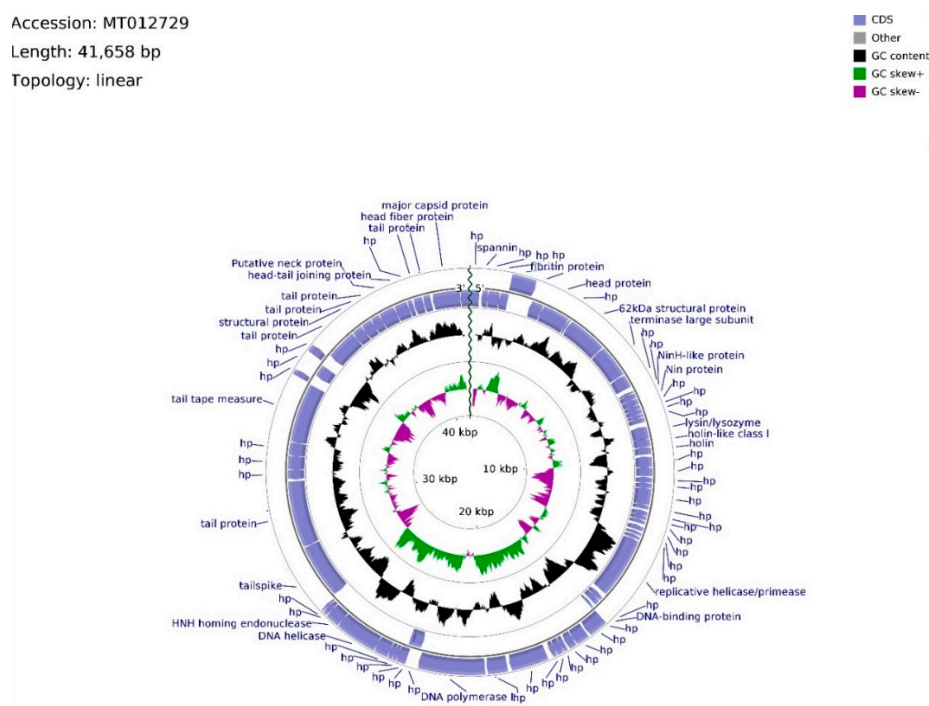


**Figure 5.** A schematic linear map of phage vB\_Sen-TO17 genome (ends of the genome are indicated by the wavy line). The inner rings show genome location, GC skew + (green) and – (purple) and GC content (black). Two the most external rings show identified open reading frames (blue arrows) and results of genome annotation process.

Twenty ORFs are spread out on the leading strand, whereas the majority (55) of ORFs are located on the complementary strand. ATG codon predominates among start codons (70 cases), whereas GTG and TTG occur 3 and 2 times, respectively. ORFs initiating with GTG and TTG codons, with the

exception of vB\_SenTO17\_45 (696 bp), have sequence spans  $\leq 144$  bp, where the average length of sequence in the vB\_Sen-TO17 genome is 535 bp. ATG codon is utilized in every ORF with an assigned function. The frequency of observed stop codons is set out as follows: TAA—40, TGA—28, TAG—7. ORFs were divided into four functional groups due to the assigned functions of their putative products: Morphogenesis (15), DNA replication (4), lysis (3), and DNA packing (2). The total number of ORFs in functional groups was excessive due to the domain determination of hypothetical proteins. In consequence, putatively protein-encoding vB\_SenTO17\_52, bearing the HNH endonuclease domain sequence, was classified within the DNA replication functional group, joined with vB\_SenTO17\_34, vB\_SenTO17\_36, vB\_SenTO17\_46, and vB\_SenTO17\_53, encoding helicase/primase, DNA-binding protein, DNA polymerase I, and DNA helicase (which start codon overlaps vB\_SenTO17\_52 stop codon), respectively. DNA replication genes are spread within the 12,966–25,568 bps span. The majority of ORF coding proteins putatively engaged in morphogenesis are located downstream, within the 26,354–41,287 bps region, with the exception of genes encoding fibrin (vB\_SenTO17\_06), putative head protein (vB\_SenTO17\_07), and 62 kDa structural protein (vB\_SenTO17\_09), located at the 2282–5401 bps region. Numerous possible transcription promoters were registered on the complementary strand in the morphogenesis-related region, in relation to the whole genome. The morphogenesis group consists mostly of genes coding for proteins involved in tail assembly (vB\_SenTO17\_07, vB\_SenTO17\_57, vB\_SenTO17\_58, vB\_SenTO17\_62, vB\_SenTO17\_66, vB\_SenTO17\_68, vB\_SenTO17\_69, vB\_SenTO17\_73), head (vB\_SenTO17\_74, vB\_SenTO17\_75), head–tail joining proteins (vB\_SenTO17\_70, vB\_SenTO17\_71), and structural proteins (vB\_SenTO17\_09, vB\_SenTO17\_67). Coding DNA Sequences (CDSs) corresponding to lysis proteins are located upstream of the DNA replication span, and occupy positions at 8694–9739 bps. They include ORFs for lysin/lysozyme (vB\_SenTO17\_19), putative holin-like class I (vB\_SenTO17\_20), and putative holin (vB\_SenTO17\_21). Nevertheless, based on nucleotide sequence analysis using the PHACTS algorithm, phage lifestyle was non-confidently classified as temperate. DNA packing CDSs are located within the 5418–6641 bps region, and the 25,565–26,062 bps span consists of genes putatively encoding the terminase large subunit (vB\_SenTO17\_10) and the HNH homing endonuclease (vB\_SenTO17\_54). Li's method analysis suggested that phage vB\_Sen-TO17 genome is packaged according to the PAC system. Following ORFs: vB\_SenTO17\_54, vB\_SenTO17\_53, and vB\_SenTO17\_46 are the only sequences located on the leading strand which may code for proteins with the reported function.

The genome of phage vB\_Sen-E22 (whole sequence deposited in GenBank; accession no. MT311645) consists of 108,987 bp, with overall GC content of 39.21% and linear topology (Figure 6). Determination of ORFs distinguished 158 putative protein-coding genes where 114 were located on the leading strand and 44 were located on the complementary strand. The frequency of start codons is set out as follows: ATG—147, GTG—8, TTG—3. Among termination codons, nucleotide triplet frequencies were set as follows: TAA—124, TGA—25, TAG—8. The functions of 67 ORFs were assigned, whereas 91 remain hypothetical. ORFs with assigned functions were divided into four functional groups: Morphogenesis (22), DNA packing (10), DNA replication (7), and lysis (2). Morphogenesis CDSs are concentrated inside the region of 46,010–74,545 bps, with nine sequences interspersed throughout the vB\_Sen-E22 genome, mainly coding for tail-related proteins with the exception of head assembly proteins vB\_SenE22\_68 and vB\_SenE22\_131. CDSs engaged in tail protein assembly dominate this genome region (11 CDSs), whereas two head-related CDSs, coding for portal protein (vB\_SenE22\_100) and major head protein precursor (vB\_SenE22\_103), are also present there. Phage head putative genes are located within the 50,510–54,248 bps span which is intersected with the tail fibers protein putative gene (vB\_SenE22\_101) and the sequence putatively encoding prohead protease (vB\_SenE22\_102). DNA packing genes are spread across the vB\_Sen-E22 genome, and they include genes encoding putative nucleases: Endonucleases (vB\_SenE22\_99, vB\_SenE22\_120, vB\_SenE22\_123, vB\_SenE22\_153), exonucleases (vB\_SenE22\_12, vB\_SenE22\_112), and ribonuclease H (vB\_SenE22\_158).



Accession: MT311645

Length: 108,987 bp

Topology: linear

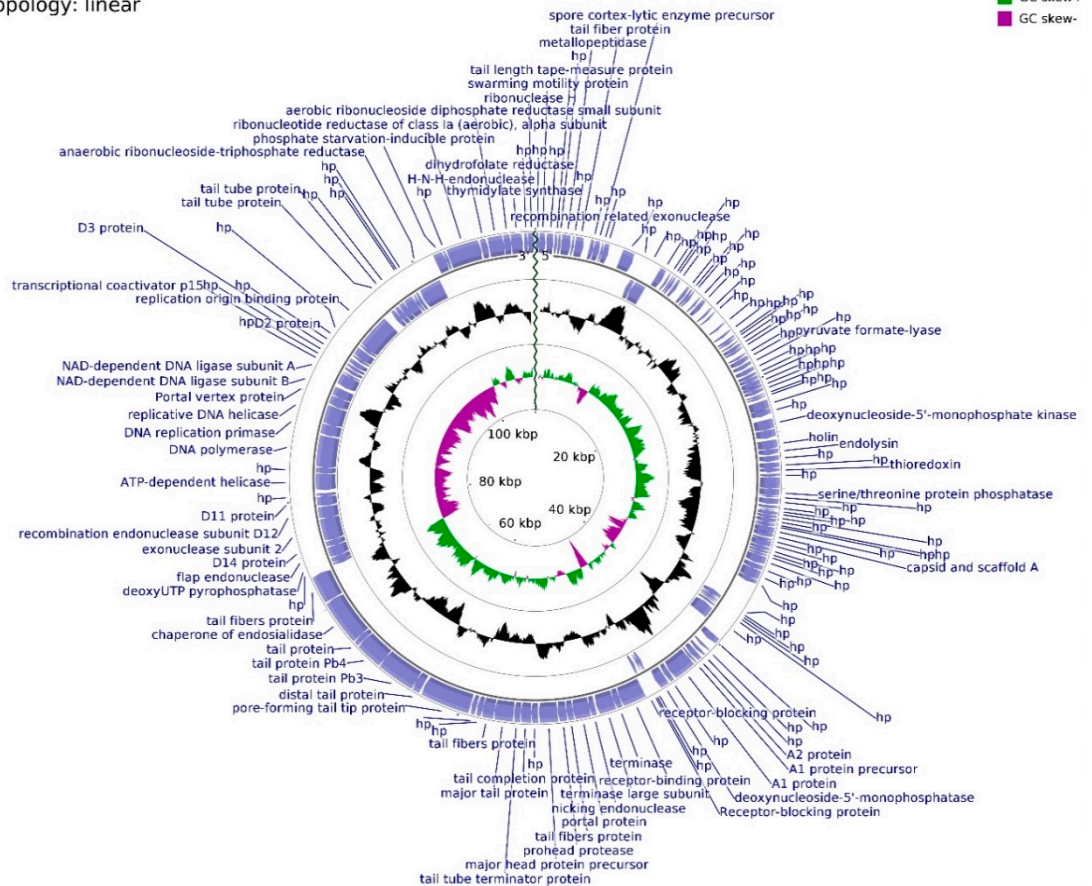


**Figure 6.** Schematic linear map of phage vB\_Sen-E22 genome (ends of the genome are indicated by the wavy line). The inner rings show genome location, GC skew + (green) and – (purple) and GC content (black). The two most external rings show identified open reading frames (blue arrows) and results of genome annotation process.

Apart from ORF for potential nicking endonuclease (vB\_SenE22\_99), two terminase subunit ORFs are situated on the leading strand which are preceded by CDSs of three receptor-blocking proteins. Using Li's method, the DNA packaging of this phage can be suggested as operating by the COS mode. ORF for recombination-related exonuclease (vB\_SenE22\_12) is located upstream of the one for the hypothetical protein bearing PHB domain putatively engaged in phage decision between lytic and lysogenic growth. Within this domain, a Rho-independent terminator is located between vB\_SenE22\_12 and vB\_SenE22\_13 CDSs. The gap of the non-coding region encompasses 943 bps, whereas the average length of a gap between coding DNA sequences across the genome is equal to 93 bps. ORFs coding for proteins putatively involved in the process of DNA replication, located on the complementary strand, are assembled in a tile-like manner at the 80,720–90,335 bps region, with the putative replication origin binding protein ORF (vB\_SenE22\_141) situated upstream of the CDS conglomerate. vB\_SenE22\_141 (93,024–95,813 bp) overlaps with the vB\_SenE22\_140 hypothetical protein gene, bearing two transcription terminators starting at positions 117 bp and 183 bp inside the 234 bps long CDS. A transcription terminator can also be found within vB\_SenE22\_141 CDS, and downstream from the DNA ligase subunit B gene (vB\_SenE22\_132), which overlaps the A subunit ORF (vB\_SenE22\_133). The DNA replication tile is interlaced with the ORF encoding uncharacterized protein and the Portal vertex (vB\_SenE22\_131), belonging to the morphogenesis functional group. Between those sequences, there are ORFs for DNA helicase, DNA replication primase, and DNA

polymerase, which are probably transcribed as two operons, as suggested by an overlap between start and stop codons with a 62 bps gap between vB\_SenE22\_129 and vB\_SenE22\_128. Based on the sequence analysis with PHACTS, this phage was non-confidently classified as lytic. Putative holin and endolysin CDSs (vB\_SenE22\_50 and vB\_SenE22\_51, respectively), representing genes coding for proteins involved in host cell lysis, overlap at positions 24,499–25,565 bps, shifting the probability of the lifestyle classification.

### 2.7. Phylogenetic Analyses

Comparisons of organizations of genomes of phages vB\_Sen-TO17 and vB\_Sen-E22 to genomes of the most related bacteriophages (according to DNA sequence similarities of whole genomes) are indicated as EasyFig in Figure 7.

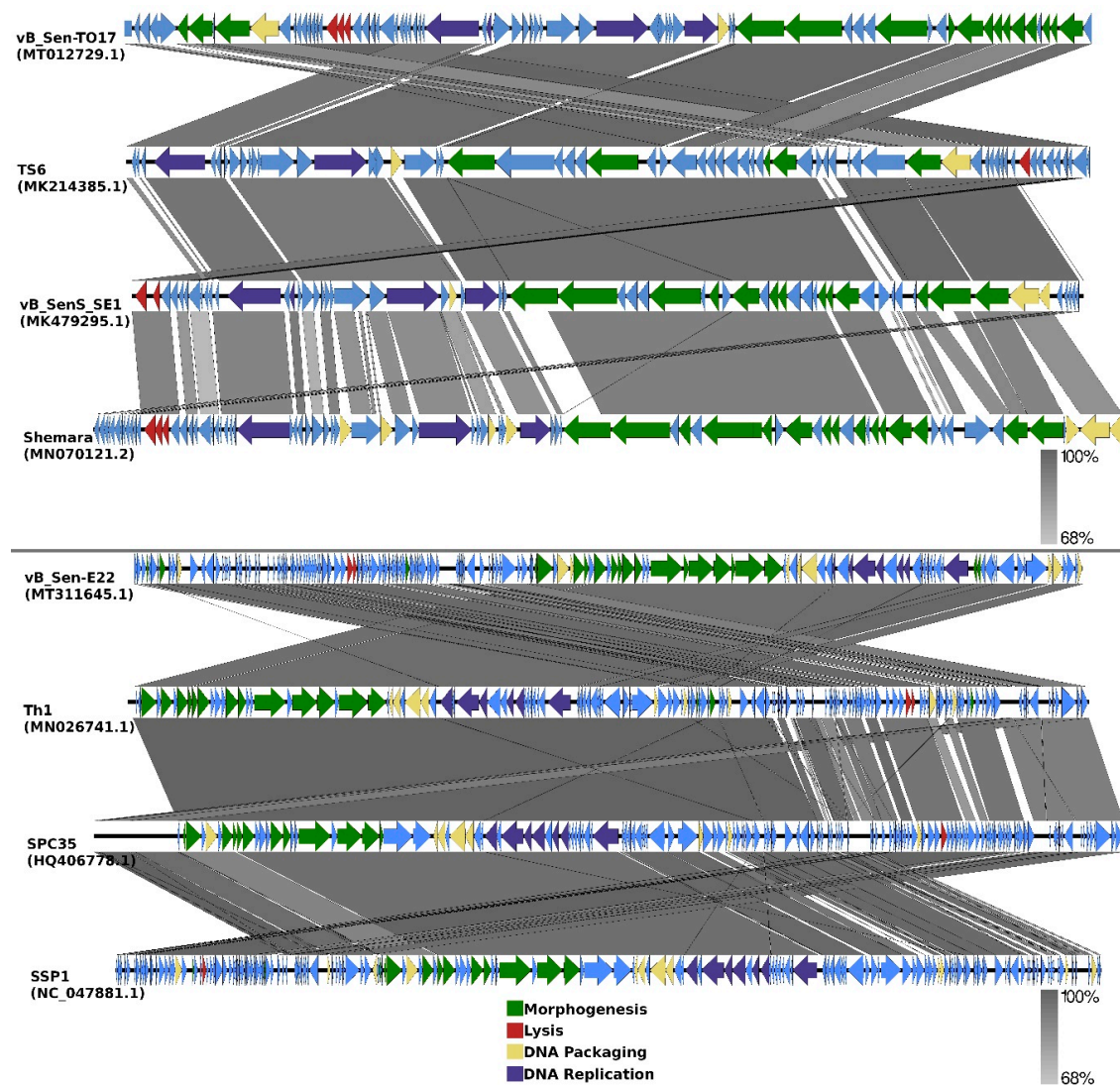


**Figure 7.** EasyFig output image of the genomic comparison between phages vB\_Sen-TO17 and vB\_Sen-E22, and the most closely related phages. Phage genomes are presented by linear visualization with coding regions shown as arrows. Selected open reading frames are colored in relation to their functions. The percentage of sequence similarity is indicated by the intensity of the gray color.

To analyse phylogenetic relationships between phage vB\_Sen-TO17 and other viruses, we have compared the nucleotide sequences of the gene of the terminase large subunit and the nucleotide

sequences of two additional markers such as genes encoding the portal protein and the major capsid protein of vB\_Sen-TO17 with the respective sequences of other phages (Figure 8). The use of only the large terminase subunit gene sequence was insufficient to show the actual phylogenetic position of vB\_Sen-TO17. The analysis of the nucleotide sequence of the gene coding for portal protein indicated that phage vB\_Sen-TO17 is a sister to phage vB\_SenS\_SE1 (MK479295.1) with high bootstrap support (BS = 99). On the other hand, as shown in Figure 8, the analysis of the major capsid protein gene together with the combined analysis of three marker genes' sequences (*TLS*, *PP*, *MCP*) indicated a close relationship of vB\_Sen-TO17 to phages vB\_SenS\_SE1 (MK479295.1) and TS6 (MK214385.1) with high bootstrap support of BS = 90 and BS = 96, respectively. Both phages belong to the family *Siphoviridae*, genus *Cornellvirus*. Sequence similarity searches of these phages demonstrated very high level of genome sequence identity with vB\_Sen-TO17 (~96% and ~98%, respectively). The above results were confirmed by the whole-genome phylogenetic analysis and the whole-genome alignments constructed using the Mauve algorithm (see Section 4.15 for details), which indicated a high level of homology between these genomes (Figure 8). Nevertheless, one should note some differences in the trees topology obtained with the use of various methods presented above, for example in the position of Shemara phage (MN070121.2).

To analyse phylogenetic relationships between phage vB\_Sen-E22 and other viruses, we compared the nucleotide sequence of the gene coding for the large terminase subunit of vB\_Sen-E22 with the sequences of genes of the large terminase subunit of other phages. As shown in Figure 9, the sequence of the large terminase subunit gene of vB\_Sen-E22 indicates its relationship to *Shigella* phage SSP1 (NC\_047881.1) with low bootstrap support BS = 63. On the other hand, the sequence similarity searches revealed that these phages show a very high level of genome sequence identity (~97%). The whole genome sequence analysis indicated that the phage vB\_Sen-E22 is a sister to the phages Th1 (NC\_048795.1) and SPC35 (HQ406778.1), with the highest BS = 100 in both cases (Figure 9). Phages SSP1, Th1, and SPC35 belong to the family *Demereciviridae*, genus *Tequintavirus*. Sequence similarity searches between Th1, SPC35, and phage vB\_Sen-E22 demonstrated a very high level of identity (~97% when comparing vB\_Sen-E22 with Th1, and ~96% when comparing vB\_Sen-E22 with SPC35). The whole-genome alignments constructed using the Mauve algorithm (see Section 4.15 for details) also revealed a high level of homology between these genomes (Figure 9). Therefore, for vB\_Sen-E22, the single marker gene phylogenetic analysis was insufficient and did not reflect the actual genetic position of this phage, probably due to mosaicism of phage genomes and a horizontal gene transfer. Nevertheless, the whole genome sequence phylogenetic analysis allowed us to obtain reliable results, leading to the proposal that vB\_Sen-E22 belongs to the family *Demereciviridae*, genus *Tequintavirus*.

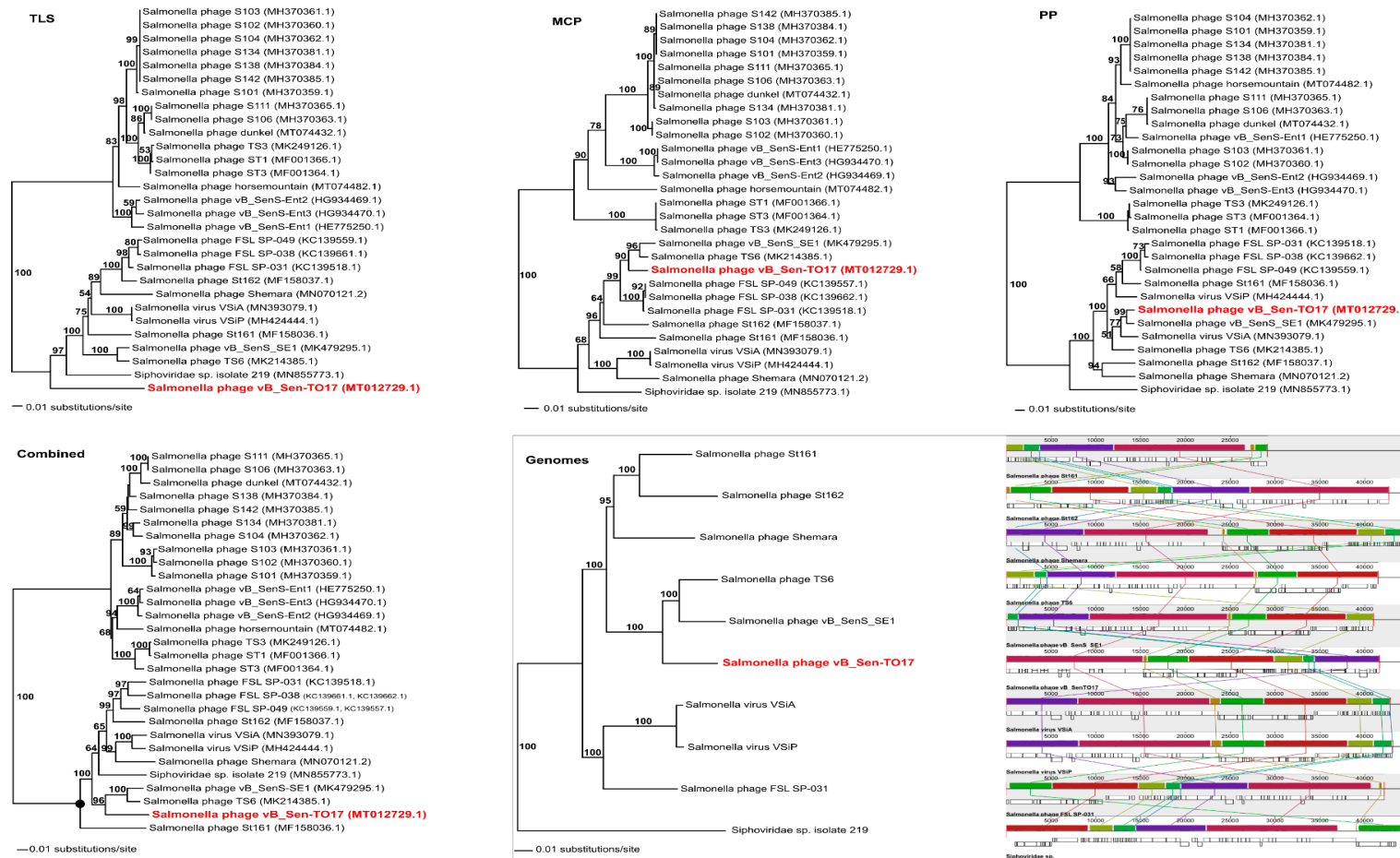


**Figure 8.** Neighbour-joining phylogenetic trees showing the phylogenetic position of phage vB\_Sen-TO17 (in red color) within Cornellvirus based on the sequences coding for terminase large subunit (TLS), major capsid protein (MCP), portal protein (PP), their combined nucleotide sequences (Combined), as well as on the whole-genome analysis (Genomes). The reference sequences were collected from the NCBI database. The tree was constructed using PAUP \*. Bootstrap value > 50%, calculated based on 1000 resamplings, is shown above the branches.

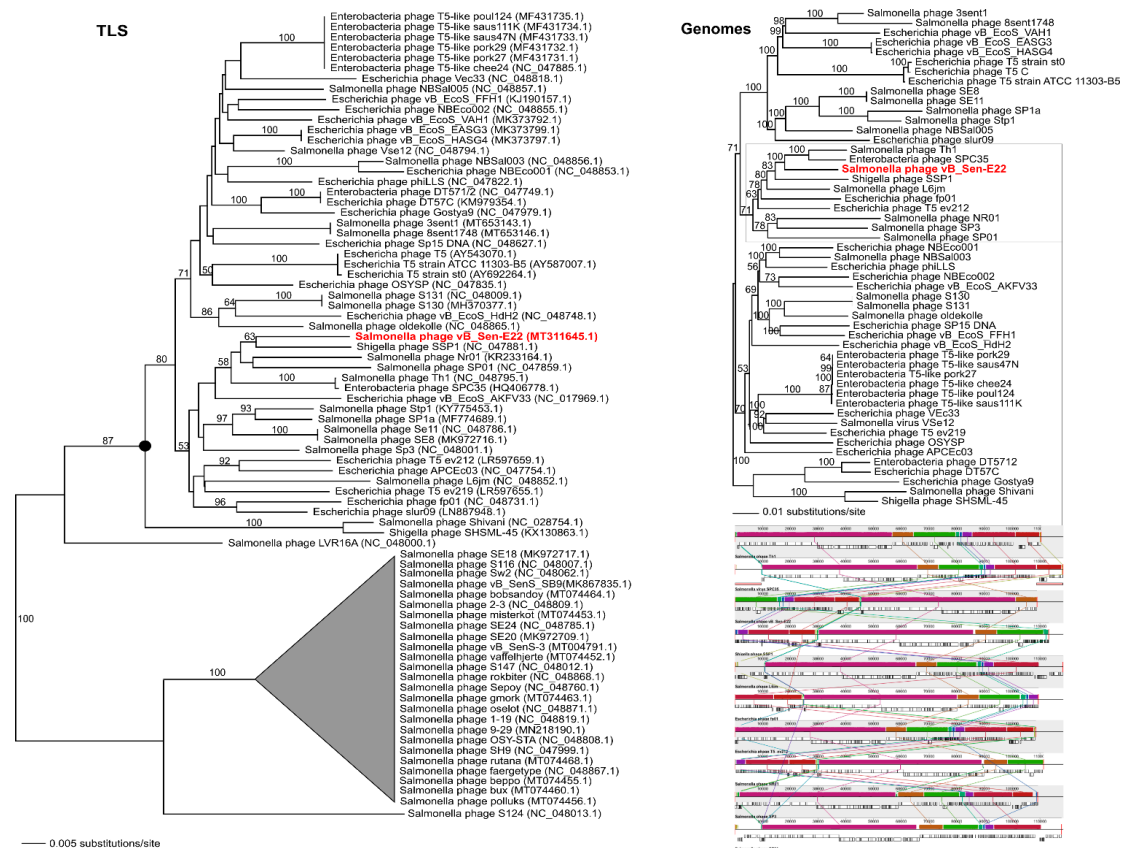


**Figure 9.** Neighbour-joining phylogenetic tree showing the phylogenetic position of phage vB\_Sen-E22 (in red color) within Tequintavirus, based on the sequence coding for terminase large subunit (TLS), as well as on the whole-genome analysis (Genomes). The reference sequences were collected from the NCBI database. The tree was constructed using PAUP\*. Bootstrap value > 50%, calculated based on 1000 resamplings, is shown above branches.

### 3. Discussion

Among foodborne pathogens, *S. enterica* is one of the most frequently occurring infectious agents, and a majority of infections arise from contamination of poultry-derived products [1,2]. Antibiotic resistance occurs commonly in this bacterium; thus, alternative methods of eradication of this pathogenic microorganism are required [3]. One might consider that anti-*Salmonella* phage therapy could be a potential option to eliminate *S. enterica* from poultry, including both gastrointestinal tract of birds and poultry-derived products. On the other hand, effective phage therapy requires specific conditions to be applied in practice [35]. Since each phage is specific to particular serovars or strains, a large collection of bacteriophages is required for effective phage therapy. Since temperate phages can lysogenize bacterial cells, virulent bacteriophages are preferred to eradicate pathogenic bacteria. It is also crucial that genomes of bacteriophages used in phage therapy are devoid of any genes coding for toxins or other proteins which are detrimental for humans or animals. Finally, phages revealing rapid and effective development are preferred in phage therapy as they may eliminate target bacteria in a relatively short time. Therefore, isolation and characterization of a large set of different bacteriophages infecting *S. enterica* is desirable if phage therapy against this bacterium can be used in practice.

In this report, we describe isolation and characterization of two bacteriophages infecting *S. enterica*. The viruses (named vB\_Sen-TO17 and vB\_Sen-E22) were newly isolated from chicken feces and both molecular and functional characterization has been performed. Despite considerable differences in their genomes, including various sizes (41,658 bp for vB\_Sen-TO17 and 108,987 bp for vB\_Sen-E22) and organizations (Figure 7), both phages do not encode any homologs of known toxins or toxin

motifs, reveal effective adsorption on host cells, and develop effectively in *S. enterica* cells giving burst sizes between 9 and 79 PFU/cell, depending on the host strain, at 42 °C (a temperature resembling that occurring naturally in chicken body). Moreover, their virions are relative stable under various conditions, including low pH (Table 3), presence of various solvents (Table 4) and different temperatures (Table 5). Although host ranges of tested phages are different, when considered together, their spectrum of sensitive *S. enterica* serovars is relatively large (Table 2). These features predispose vB\_Sen-TO17 and vB\_Sen-E22 to be used in phage therapy procedures.

Despite vB\_Sen-E22 genome is about 2.6 times larger than that of vB\_Sen-TO17 (108,987 bps vs. 41,658 bps), a diameter of the head of the former phage is only 10 nm bigger than that of the latter virus (58 vs. 48 nm). Nevertheless, when calculating volumes of heads of these bacteriophages, one can estimate that they are about 101.8 thousand nm<sup>3</sup> and about 57.7 thousand nm<sup>3</sup> for vB\_Sen-E22 and vB\_Sen-TO17, respectively. Therefore, the genome of vB\_Sen-E22 must be only moderately more densely packaged inside the head than that of vB\_Sen-TO17.

Genomic analyses, performed with using the PHACTS algorithm (see Section 4.14), suggested that vB\_Sen-TO17 might be a temperate phage. On the other hand, absence of genes with clear homology to those coding for integration and immunity proteins makes such a possibility doubtful. Moreover, the prediction that this might be a temperate phage was not confirmed by experimental results. The vB\_Sen-TO17 virus forms clear plaques (Figure 1 and Table 1) and was found to be unable to lysogenize host cells under laboratory conditions. Therefore, we assume that a halo visible around plaques of this phage may arise from activities of lytic enzymes which if released from lysed cells and remaining relatively stable in the agar, might cause inhibition of growth of uninfected bacteria neighboring lysed ones. Since vB\_Sen-TO17 encodes 3 lytic enzymes, lysin/lysozyme (vB\_SenTO17\_19), putative holin-like class I (vB\_SenTO17\_20), and putative holin (vB\_SenTO17\_21), such hypothesis appears to be of high probability. Therefore, we conclude that it is a virulent rather than temperate phage, while genomic analyses might indicate features of its ancestors, and corresponding genes may be either inactive now or play different roles in phage development.

Bacteriophage vB\_Sen-E22 also forms clear plaques but without halo (Figure 1 and Table 1). Moreover, its genome is characteristic for virulent phages, confirming that this virus is unable to form prophages in infected bacteria.

Molecular phylogenetic studies were somewhat complicated in the case of vB\_Sen-TO17, as the analysis of the gene encoding large terminase subunit (classical molecular marker for such analyses in studies on bacteriophages) was not sufficient to determine the actual phylogenetic position of this phage. Nevertheless, comparisons of sequences of two additional genes allowed us to indicate that vB\_Sen-TO17 is closely related to two other phages, vB\_SenS\_SE1 and TS6, which belong to the family *Siphoviridae* and genus *Cornellovirus*. Since sequence similarity searches indicated a high level of identity to vB\_Sen-TO17, about 96% and about 98%, respectively, we propose to classify the newly isolated phage to family *Siphoviridae* and genus *Cornellovirus*. This conclusion was corroborated by whole-genome phylogenetic analysis.

Phylogenetic analyses of vB\_Sen-E22 were also not obvious and easy, as similarity of its large terminase subunit gene did not reveal high identity with any other phage. The analyses indicated its relationship to *Shigella* phage SSP1; however, the bootstrap support was relatively low (BS = 62). Nevertheless, since whole genome sequence identity between these two phages is at the level of 97%, and such a level of similarity occurs also when comparing two other phages closely related to vB\_Sen-E22, Th1, and SPC35, which belong to family *Demereciviridae* and genus *Tequintavirus*, we propose to classify vB\_Sen-E22 to the same family and genus.

In conclusion, our studies, presented in this report, indicate that newly isolated and characterized bacteriophages vB\_Sen-TO17 and vB\_Sen-E22 can be used for further studies on anti-*Salmonella* phage therapy, particularly for eradication of *E. enterica* from poultry.

## 4. Materials and Methods

### 4.1. Bacterial Strains

Strains of *S. enterica*, used in this study, come from the National Salmonella Center at Medical University of Gdansk (Gdansk, Poland). Strains of *Proteus vulgaris*, *Citrobacter freundii*, *Enterococcus faecalis*, and *Escherichia coli* come from the Department of Molecular Biology of the University of Gdansk collection of microorganisms (Gdansk, Poland). *Staphylococcus aureus* strain 6538<sup>TM</sup>, *Lactococcus lactis* 49032<sup>TM</sup> and *Lactobacillus acidophilus* 314<sup>TM</sup> come from ATCC.

### 4.2. Bacterial Culture Conditions

Bacteria were cultured at 37 °C or 42 °C. LB-medium (BioShop, Burlington, ON, Canada) was used to cultivate Gram-negative bacteria. For *S. aureus*, *E. faecalis*, *L. lactis*, and *L. acidophilus*, a BHI medium (Graso Biotech, Starogard Gdański, Poland) was used. Bacteriological agar (BioShop, Burlington, ON, Canada) at a final concentration of 1% was used in solidified media (LB-agar or BHI-agar). *L. lactis* and *L. acidophilus* were cultivated under microaerophilic conditions using the GenBox microaer system (BioMérieux, Marcy l'Etoile, France).

### 4.3. Isolation and Purification of Phages *vB\_Sen-TO17* and *vB\_Sen-E22*

Chicken feces were suspended in an LB medium at a 1:10 ratio, homogenized using hand homogenizer (GenoPlast Biochemicals, Rokocin, Poland), and incubated overnight at 37 °C (Heraeus B-12, Kendro Laboratory Products, Langensfeld, Germany). The samples were then centrifuged at 6000× g for 20 min at 4 °C (Avanti JXN-26, rotor JS-13.1, Beckman Coulter, Indianapolis, USA), and supernatants were collected and filtered through a 0.22 µm syringe filter (Millex-GP, Sigma-Aldrich, USA). Ten-fold dilutions were prepared in an LB medium and 100 µL of each dilution was mixed with 200 µL of bacterial host culture and 4 mL of LB with 0.7% agar. The mixture was poured onto plates containing 20 mL of LB-agar. The double-layer agar plates were incubated at 42 °C (BF 53, BINDER GmbH, Tuttlingen, Germany) overnight and then scanned for plaques. Different looking plaques were then collected, transferred to 10 mL of freshly diluted (1:100 ratio) host strain culture, and incubated with shaking at 155 rpm for 3 h at 42 °C (OLS 200, Grant Instruments, Sherepeth, UK). Obtained lysates were treated with 5 mL chloroform (Alchem, Torun, Poland), centrifuged (4000× g, 10 min, 4 °C), and filtered through 0.22 µm filter. The lysates were then titrated on double-layer agar plates. The plates were incubated overnight at 42 °C and then scanned for uniform plaques. The purity of lysates was also checked using electron microscopy.

### 4.4. Phage Propagation

A 10 mL amount of bacterial host culture, grown overnight in LB medium, was added to 1 L of LB and incubated at 37 °C with agitation at 150 rpm. At OD<sub>600</sub> = 0.15 (measured by using SmartSpec PLUS, BIO-RAD, CA, USA) bacteria were infected with phages at a multiplicity of infection (m.o.i.) of 0.5 and incubated at 37 °C until lysis occurred. For phage purification, polyethylene glycol (PEG) 8000 (BioShop, Burlington, Ontario, Canada) was added to the final concentration of 10% and stirred (Carl Roth, Karlsruhe, Germany) overnight at 4 °C. The precipitate was collected by centrifugation at 10,000× g for 30 min at 4 °C (Avanti JXN-26, rotor JLA-8000, Beckman Coulter, IN, USA) and suspended in 0.89% NaCl (Alchem, Torun, Poland). PEG 8000 was removed by adding 2 mL of chloroform and centrifugation at 4000× g for 15 min at 4 °C (Avanti JXN-26, rotor JS-13.1, Beckman Coulter, IN, USA). The procedure was repeated until no PEG 8000 precipitate could be observed.

### 4.5. Electron Microscopy

Phages were purified by centrifugation using CsCl (Sigma Aldrich, MO, USA) density gradient as described previously [36]. Transmission electron microscopy analysis of phage capsids was performed

in the Laboratory of Electron Microscopy, Faculty of Biology, University of Gdansk, Gdansk, Poland. Virions were negatively stained with uranyl acetate (VWR International Ltd., Radnor, PA, USA) and then micrographs were taken under a Tecnai G2 Spirit BioTWIN electron microscope (FEI, Thermofisher Scientific, OR, USA).

#### 4.6. Plaque Morphology Assessment

The plaque morphology analysis of bacteriophages was performed using *S. Typhimurium* 13 as a host. Ten-fold dilutions of phage lysate were prepared in 0.89% NaCl; 200  $\mu$ L of overnight host culture were mixed with 10  $\mu$ L of an appropriate dilution of phage lysate and added to 4 mL of LB with 0.7% agar. The mixture was poured onto plates containing 20 mL of LB agar. The double-layer agar plates were incubated at 42 °C for 16 h. Plaque morphology and diameter were determined.

#### 4.7. Determination of Phage Host Range and Efficiency of Lysogenization

Host range of bacteriophages was determined using the spot-test method described previously [34], with some modifications. Ten-fold dilutions of phage stocks were prepared in 0.89% NaCl; 10  $\mu$ L of the appropriate dilution was mixed with 200  $\mu$ L of overnight bacterial culture and 4 mL of LB with 0.7% agar. Plates were incubated overnight at 37 °C and then scanned for plaques.

For lysogenization experiments, *S. Agona* 1408, *S. Dublin* 65, *S. Enteritidis* 64, *S. Enteritidis* 1392, *S. Heidelberg* 16, *S. Infantis* 165, *S. Newport* 50, *S. Typhimurium* 12, *S. Typhimurium* 13, and *S. Virchow* 41 were cultivated to  $OD_{600} = 0.2$  at 42 °C. Then, a sample of 1 mL of bacterial culture was centrifuged (2000 $\times$  g, 10 min, 4 °C) and the pellet was resuspended in 1 mL of 0.5  $\times$  LB medium. Following incubation for 5 min at 30 °C, phage lysate was added to m.o.i. = 1. In the control variant of the experiment, 0.5  $\times$  LB was added instead of phage lysate. Bacteria were incubated for 3 h at 30 °C, and then centrifuged (4000 $\times$  g, 5 min, 4 °C) in order to remove free phage particles. Supernatant was discarded, and the pellet was resuspended in a fresh LB medium. Serial dilutions were prepared in 0.89% NaCl and 30  $\mu$ L of each dilution was spread onto LB plates. After 24 h incubation at 30 °C, 96 colonies were passaged separately, each in a well of a 96-well plate with 150  $\mu$ L of LB medium. The plates were incubated with shaking at 42 °C until bacteria culture reached  $OD_{600} = 0.2$ .

For estimation of efficiency of lysogenization, mitomycin C was added (to a final concentration of 1  $\mu$ g/mL) to 150  $\mu$ L of bacterial culture derived from a single tested colony (this antibiotic had been demonstrated previously to induce prophages in *S. enterica* [37–39]). The plates were then incubated for 3 h. Afterwards, 10  $\mu$ L of chloroform was added, the plates were centrifuged (2000 $\times$  g, 10 min, 4 °C), and 5  $\mu$ L of water phase was spotted onto double-layer LB agar plates. The plates were incubated overnight at 42 °C and then scanned for plaques. A colony was determined as lysogenic if plaques were formed on bacterial lawn. The efficiency of lysogenization was determined as a percent of lysogens among all tested bacterial colonies. The experiment was performed in triplicate.

In order to test the resistance to superinfection, 50  $\mu$ L of bacterial culture was mixed with 4 mL of 0.7% LB agar and poured onto an LB agar plate. Then, 2.5  $\mu$ L of phage lysate was spotted on top of it. The plates were incubated overnight at 42 °C and scanned for plaques. If plaques were not visible, the clone was recognized as resistant to phage. The resistance to infection was determined as a percent of bacteria not infected by the phage. The experiments were performed in triplicates.

#### 4.8. Phage Sensitivity to Various Conditions

Sensitivity of phages to low pH conditions was performed as described previously [21]. Briefly, 100  $\mu$ L of phage lysate were added to 900  $\mu$ L of LB at pH 1.8, 2.0, 2.2, 2.5, 2.8, 3.0, 10.0, and 12.0, with pH 7.0 used as a control variant. The pH was adjusted by addition 1 M HCl (Alchem, Torun, Poland) or 1 M NaOH (Alchem, Torun, Poland) and measured using a pH meter (pH 50+ DHS, Giorgio Bormac, Carpi, Italy). Samples were mixed and incubated for 1 h at 42 °C. Afterwards, samples were serially diluted and overlaid on top of LB agar plates with the top agar containing 200  $\mu$ L of overnight bacterial culture. Plates were incubated overnight at 37 °C and then scanned for plaques. Susceptibility



to disinfectants, liquid media, and buffers were performed in accordance with a procedure described previously [34,37]. Briefly, 100  $\mu$ L of phage lysate was added to 900  $\mu$ L of tested solution. The samples were mixed and incubated for 1 h at 25 °C or for 24 h at 37 °C for DMEM (Thermo Fisher Scientific Inc., Paisley, UK), supplemented with 10% fetal bovine serum (Thermo Fisher Scientific Inc., Paisley, UK) and 1% antibiotic/antimycotic solution (Sigma Aldrich Co. LLC., St. Louis, MO, USA). The experiments were performed in triplicates.

#### 4.9. Phage Sensitivity to Different Temperatures

Phage survivability at different temperatures was assessed in accordance with previously described protocol [34]. Phages were diluted in 0.89% NaCl to a final concentration of  $10^9$  PFU/mL and then incubated at temperature  $-80$  °C (Revco ULT-1790-10V, Thermo Fisher Scientific, OR, USA),  $-20$  °C,  $4$  °C,  $25$  °C,  $37$  °C,  $42$  °C,  $60$  °C, or  $95$  °C for a given period of time. Following the incubation, 10-fold dilutions were prepared in 0.89% NaCl and overlaid on top of double agar plates. The plates were incubated at  $42$  °C overnight and then scanned for plaques. The percent of surviving phages was calculated as a ratio of surviving phages to phage titer before incubation. The experiments were done in triplicates.

#### 4.10. Efficiency of Phage Plating at Different Temperatures

The analysis of phage titration dependence on temperature was performed in accordance with previously described protocol [34]. Briefly, 10-fold dilutions of phage lysates were prepared in 0.89% NaCl and overlaid on top of double agar plates. The plates were incubated at  $20$  °C,  $25$  °C,  $37$  °C, and  $42$  °C overnight. The efficacy of phage plating was assessed by comparison of phage titers obtained at different temperatures. The experiments were performed in triplicates.

#### 4.11. Efficiency of Phage Adsorption

An adsorption assay was performed according to the protocols described previously [40], with some modifications. Overnight cultures of bacterial strains were diluted 1:100 in fresh LB medium and incubated with shaking at  $42$  °C until  $OD_{600} = 0.2$  was reached. Then, 2 mL samples were centrifuged at  $2000\times g$ , 5 min,  $4$  °C (MiniSpin Plus, Eppendorf, Hamburg, Germany) and the pellet was suspended in 1 mL of fresh LB medium. After 10 min incubation at  $42$  °C, phages were added to final m.o.i. of 0.1. At given time points, 100  $\mu$ L samples were collected and centrifuged at  $6000\times g$  for 30 s. Ten-fold dilutions were prepared and overlaid on top of double-layer agar plates containing 0.7% LB agar with 200  $\mu$ L of bacterial host culture. The number of viruses mixed with bacterial host cells at time 0 was considered 100% non-adsorbed phages. Other values were compared to this sample. The experiment was performed in triplicates.

#### 4.12. One-Step Growth Experiments

One-step growth experiments were performed as described previously [21], with some modifications. Bacteria were grown at  $42$  °C until reaching optical density of  $OD_{600} = 0.1$ . Then, 10 mL of bacterial culture were centrifuged ( $4000\times g$ , 10 min,  $4$  °C) (Avanti JXN-26, rotor JS-13.1, Beckman Coulter, Indianapolis, USA), and the pellet was suspended in 1 mL of LB medium at  $4$  °C. Phages were added to the host culture at m.o.i. = 0.1 and allowed to adsorb for 5 min at  $42$  °C. The mixture was centrifuged at  $4,000\times g$  for 10 min at  $4$  °C to remove unadsorbed phage particles. After centrifugation, 50  $\mu$ L of phage-bacteria mixture was added to 20 mL of LB medium (time 0) and cultivated at  $42$  °C. The number of infective centers was estimated from samples taken 1 min, 2.5 min, and 5 min after infection, by mixing 10  $\mu$ L of sample with 200  $\mu$ L of overnight bacterial culture and 4 mL of 0.7% LB agar. Samples (100  $\mu$ L each) were collected at given temperatures, mixed with 50  $\mu$ L of chloroform, cleared by centrifugation ( $6000\times g$ , 30 sec) (MiniSpin Plus, Eppendorf, Hamburg, Germany), and titrated to determine the number of PFU/mL. Simultaneously, 100  $\mu$ L samples were collected, centrifuged immediately ( $6000\times g$ , 30 s), and titrated. The plates were incubated at  $42$  °C overnight. The experiment

was performed in triplicates. Burst size was calculated as the ratio of phage titer from samples untreated with chloroform to the number of infection centers. Total phage yield was calculated as the ratio of phage titer from chloroform-treated samples to the number of infection centers.

#### 4.13. Phage DNA Isolation

Phage lysate, purified as described in Section 4.5, was treated with DNase I (1 U/ $\mu$ L; Thermo Fisher Scientific Inc., Paisley, UK) and RNase A (5  $\mu$ g/ $\mu$ L; Thermo Fisher Scientific Inc., Paisley, UK) to degrade bacterial nucleic acids. To digest the exogenous DNA and RNA, the mixture was incubated for 30 min at 37 °C. Then, DNase I and RNase A were inactivated by heating to 95 °C and 5 min incubation. Genomic DNA of phages was isolated with a MasterPure™ Complete DNA and RNA Purification Kit (Epicentre Biotechnologies, WI, USA) in accordance with the manufacturer's guidelines.

#### 4.14. Genomic Analysis of Phages vB\_Sen-E22 and vB\_Sen-TO17

Genomes of vB\_Sen-E22 and vB\_Sen-TO17 phages were sequenced using the Whole Genome Shotgun (WGS) strategy and run on the MiSeq Illumina platform. Samples for next-generation sequencing were prepared according to the NEBNext DNA Library Prep Master Mix Set for the Illumina manual with random selection. The read length interval ranged from 36 to 251 bp. Raw reads were deposited in SRA databases under BioProject ID: PRJNA671789.

Annotation and sequence analysis was conducted as described previously [21]. Briefly, annotation was based on open reading frame prediction obtained via the RASTtk toolkit [41] and the Prokka suite containing Prodigal [42] where points of difference were settled by analysis of Ribosome Binding Sites (RBS) 4-12 nucleotides upstream of start codons. Putative functions of ORFs were assessed employing the Nucleotide Collection (nr/nt) database with the CDD database [43], 97 Salmonella phage genomes from pVOGs database (<http://dmk-brain.ecn.uiowa.edu/pVOGs/>, last accessed on 16 November 2020), and the HMMer Reference Proteomes database [44]. Phage-specific promoters were predicted by using the Neural Network Promoter Prediction NNPP method ([http://www.fruitfly.org/seq\\_tools/promoter.html](http://www.fruitfly.org/seq_tools/promoter.html), last accessed on 16 November, 2020). To find Rho-independent terminators in nucleic acid sequences, the Arnold tool was employed [45]. Classification of phages lifestyle was predicted using PHACTS [46]. For phage genome termini analysis, packing mode and topology of viral genomes PhageTerm was employed [47]. To create maps of viral genomes, the CGView Comparison Tool [48] was used, with additional GC skew and GC content analysis. Comparison of genomes of related phages was performed using the EasyFig program (<http://mjsull.github.io/Easyfig/files.html>, last accessed on 14 August 2020).

#### 4.15. Phylogenetic Analysis of Phages vB\_Sen-E22 and vB\_Sen-TO17

To estimate the phylogenetic positions of the newly isolated phages vB\_Sen-E22 and vB\_Sen-TO17, the nucleotide sequences of the terminase large subunit gene (genetic marker for the order Caudovirales) were compared with the sequences of other reference bacteriophages that were deposited in the NCBI database. We have also compared the nucleotide sequences of genes coding for major capsid protein and portal protein of vB\_Sen-TO17. DNA sequences were translated to amino acid, then aligned and adjusted by eye using Seaview [49]. Additionally, we conducted the whole-genome sequence phylogenetic analyses for both phages. Multiple genome alignments were conducted through the progressive Mauve algorithm [50]. Each subalignment generated by Mauve was adjusted by eye and concatenated using Seaview [49]. All matrices were analyzed using PAUP\* (Phylogenetic Analysis Using Parsimony\* and Other Methods) version 4.0a [51]. The optimality criterion was set to distance using the Neighbour-Joining algorithm (NJ). The p-distance was used based on a previously published recommendation [52]. The robustness of the tree topology was assessed by bootstrap analyses based on 1000 replicates.

**Supplementary Materials:** The supplementary materials are available online at <http://www.mdpi.com/1422-0067/21/22/8821/s1>.

**Author Contributions:** Conceptualization, K.K.-K., G.W. and A.W.; methodology, K.K.-K., M.G. (Michał Grabski), M.G. (Marcin Górniak), and A.J.-K.; validation, K.K.-K. and M.G. (Michał Grabski); experimental investigation, K.K.-K., Ł.G. and M.K.; data analysis, K.K.-K., M.G. (Michał Grabski), M.G. (Marcin Górniak), A.J.-K. and A.W.; data interpretation, K.K.-K., M.G. (Michał Grabski), M.G. (Marcin Górniak), A.J.-K., G.W. and A.W.; writing—original draft preparation, K.K.-K. and A.W.; writing—review and editing, K.K.-K., M.G. (Michał Grabski), G.W. and A.W.; visualization, K.K.-K., M.G. (Michał Grabski) and M.G. (Marcin Górniak); supervision, A.W.; funding acquisition, A.W. All authors have read and agreed to the published version of the manuscript.

**Funding:** This research was funded by National Science Center (Poland), grant no. 2017/27/B/NZ9/00393.

**Acknowledgments:** The authors would like to thank Magdalena Narajczyk for making electron microscopic images, and Jakub Kaźmierczak for providing software enabling phage capsid measurements and help with its use.

**Conflicts of Interest:** The authors declare no conflict of interest. The funders had no role in the design of the study; in the collection, analyses, or interpretation of data; in the writing of the manuscript, or in the decision to publish the results.

## References

- Torres-Acosta, M.A.; Clavijo, V.; Vaglio, C.; González-Barrios, A.F.; Vives-Flórez, M.J.; Rito-Palomares, M. Economic evaluation of the development of a phage therapy product for the control of *Salmonella* in poultry. *Biotechnol. Progr.* **2019**, *35*, 2852. [[CrossRef](#)]
- Clavijo, V.; Florez, M.J.V. The gastrointestinal microbiome and its association with the control of pathogens in broiler chicken production: A review. *Poult. Sci.* **2018**, *97*, 1006–1021. [[CrossRef](#)]
- Gal-Mort, O.; Boyle, E.C.; Grassl, G.A. Same species, different diseases: How and why typhoidal and non-typhoidal *Salmonella enterica* serovars differ. *Front. Microbiol.* **2014**, *5*, 391. [[CrossRef](#)]
- Davies, J.; Davies, D. Origins and evolution of antibiotic resistance. *Microbiol. Mol. Biol. Rev.* **2010**, *74*, 417–433. [[CrossRef](#)]
- Okocha, R.C.; Olatoye, I.O.; Adedeji, O.B. Food safety impacts of antimicrobial use and their residues in aquaculture. *Public Health Rev.* **2018**, *39*, 21. [[CrossRef](#)] [[PubMed](#)]
- Hutchings, M.; Truman, A.; Wilkinson, B. Antibiotics: Past, present and future. *Curr. Opin. Microbiol.* **2019**, *51*, 72–80. [[CrossRef](#)] [[PubMed](#)]
- Bengtsson, B.; Greko, C. Antibiotic resistance—Consequences for animal health, welfare, and food production. *Uppsala J. Med. Sci.* **2014**, *119*, 96–102. [[CrossRef](#)] [[PubMed](#)]
- Ventola, C.L. The antibiotic resistance crisis: Part 1: Causes and threats. *Pharm. Therapeut.* **2015**, *40*, 277–283.
- Górski, A.; Międzybrodzki, R.; Jończyk-Matysiak, E.; Borysowski, J.; Letkiewicz, S.; Weber-Dąbrowska, B. The fall and rise of phage therapy in modern medicine. *Expert Opin. Biol. Ther.* **2019**, *19*, 1115–1117. [[CrossRef](#)]
- Górski, A.; Międzybrodzki, R.; Węgrzyn, G.; Jończyk-Matysiak, E.; Borysowski, J.; Weber-Dąbrowska, B. Phage therapy: Current status and perspectives. *Med. Resr Rev.* **2020**, *40*, 459–463. [[CrossRef](#)]
- Rohde, C.; Resch, G.; Pirnay, J.P.; Blasdel, B.G.; Debarbieux, L.; Gelman, D.; Górski, A.; Hazan, R.; Huys, I.; Kakabadze, E.; et al. Expert opinion on three phage therapy related topics: Bacterial phage resistance, phage training and prophages in bacterial production strains. *Viruses* **2018**, *10*, 178. [[CrossRef](#)] [[PubMed](#)]
- Yan, T.; Liang, L.; Yin, P.; Zhou, Y.; Sharoba, A.M.; Lu, Q.; Dong, X.; Liu, K.; Connerton, I.F.; Li, J.; et al. Application of a novel phage LPSEYT for biological control of *Salmonella* in foods. *Microorganisms* **2020**, *8*, 400. [[CrossRef](#)] [[PubMed](#)]
- Kakabadze, E.; Makalatia, K.; Grdzlishvili, N.; Bakuradze, N.; Goderdzishvili, M.; Kusradze, I.; Phoba, M.F.; Lunguya, O.; Lood, C.; Lavigne, R.; et al. Selection of potential therapeutic bacteriophages that lyse a CTX-M-15 extended spectrum  $\beta$ -lactamase producing *Salmonella enterica* serovar Typhi strain from the Democratic Republic of the Congo. *Viruses* **2018**, *10*, 172. [[CrossRef](#)] [[PubMed](#)]
- Huang, C.; Virk, S.; Shi, J.; Zhou, Y.; Willias, S.P.; Morsy, M.K.; Abdelnabby, H.E.; Liu, J.; Wang, X.; Li, J.; et al. Isolation, characterization, and application of bacteriophage LPSE1 against *Salmonella enterica* in ready to eat (RTE) foods. *Front. Microbiol.* **2018**, *9*, 1046. [[CrossRef](#)] [[PubMed](#)]
- Sritha, K.; Bhat, S.G. Genomics of *Salmonella* phage  $\Phi$ Stp1: Candidate bacteriophage for biocontrol. *Virus Genes* **2018**, *54*, 311–318. [[CrossRef](#)]

16. Chen, Y.; Sun, E.; Song, J.; Tong, Y.; Wu, B. Three *Salmonella enterica* serovar Enteritidis bacteriophages from the *Siphoviridae* family are promising candidates for phage therapy. *Can. J. Microbiol.* **2018**, *6*, 865–875. [[CrossRef](#)]
17. Patil, K.; Zeng, C.; O’Leary, C.; Lessor, L.; Kongari, R.; Gill, J.; Liu, M. Complete genome sequence of *Salmonella enterica* serovar *Typhimurium siphophage* Seabear. *Microbiol. Resour. Announc.* **2019**, *8*, e01160-19. [[CrossRef](#)]
18. Holguín, A.V.; Cárdenas, P.; Prada-Peñaranda, C.; Rabelo Leite, L.; Buitrago, C.; Clavijo, V.; Oliveira, G.; Leekitcharoenphon, P.; Møller Aarestrup, F.; Vives, M.J.; et al. Host resistance, genomics and population dynamics in a *Salmonella* Enteritidis and phage system. *Viruses* **2019**, *11*, 188. [[CrossRef](#)]
19. Bao, H.; Shahin, K.; Zhang, Q.; Zhang, H.; Wang, Z.; Zhou, Y.; Zhang, X.; Zhu, S.; Stefan, S.; Wang, R.; et al. Morphologic and genomic characterization of a broad host range *Salmonella enterica* serovar Pullorum lytic phage vB\_SpUM\_SP116. *Microb. Pathog.* **2019**, *136*, 103659. [[CrossRef](#)]
20. Mohamed, A.; Taha, O.; El-Sherif, H.M.; Connerton, P.L.; Hooton, S.P.T.; Bassim, N.D.; Connerton, I.; El-Shibiny, A. Bacteriophage ZCSE2 is a potent antimicrobial against *Salmonella enterica* serovars: Ultrastructure, genomics and efficacy. *Viruses* **2020**, *12*, 424. [[CrossRef](#)]
21. Kosznik-Kwaśnicka, K.; Ciemińska, K.; Grabski, M.; Grabowski, Ł.; Górnaiak, M.; Jurczak-Kurek, A.; Węgrzyn, G.; Węgrzyn, A. Characteristics of a series of three bacteriophages infecting *Salmonella enterica* strains. *Int. J. Mol. Sci.* **2020**, *21*, 6152. [[CrossRef](#)] [[PubMed](#)]
22. Sevilla-Navarro, S.; Marín, C.; Cortés, V.; García, C.; Vega, S.; Catalá-Gregori, P. Autophagy as a control measure for *Salmonella* in laying hens. *Poult. Sci.* **2018**, *97*, 4367–4373. [[CrossRef](#)] [[PubMed](#)]
23. Tie, K.; Yuan, Y.; Yan, S.; Yu, X.; Zhang, Q.; Xu, H.; Zhang, Y.; Gu, J.; Sun, C.; Lei, L.; et al. Isolation and identification of *Salmonella pullorum* bacteriophage YSP2 and its use as a therapy for chicken diarrhea. *Virus Genes* **2018**, *54*, 446–456. [[CrossRef](#)] [[PubMed](#)]
24. Clavijo, V.; Baquero, D.; Hernandez, S.; Farfan, J.C.; Arias, J.; Arévalo, A.; Donado-Godoy, P.; Vives-Flores, M. Phage cocktail SalmoFREE® reduces *Salmonella* on a commercial broiler farm. *Poult. Sci.* **2019**, *98*, 5054–5063. [[CrossRef](#)]
25. Vaz, C.S.L.; Voss-Rech, D.; Alves, L.; Coldebella, A.; Brentano, L.; Trevisol, I.M. Effect of time of therapy with wild-type lytic bacteriophages on the reduction of *Salmonella* Enteritidis in broiler chickens. *Vet. Microbiol.* **2020**, *240*, 108527. [[CrossRef](#)]
26. Li, M.; Lin, H.; Jing, Y.; Wang, J. Broad-host-range *Salmonella* bacteriophage STP4-a and its potential application evaluation in poultry industry. *Poult. Sci.* **2020**, *99*, 3643–3654. [[CrossRef](#)]
27. Żbikowska, K.; Michalczuk, M.; Dolka, B. The use of bacteriophages in the poultry industry. *Animals* **2020**, *10*, 872. [[CrossRef](#)]
28. Nikkhahi, F.; Soltan Dallal, M.M.; Alimohammadi, M.; Rahimi Foroushani, A.; Rajabi, Z.; Fardsanei, F.; Imeni, S.M.; Torabi Bonab, P. Phage therapy: Assessment of the efficacy of a bacteriophage isolated in the treatment of salmonellosis induced by *Salmonella* Enteritidis in mice. *Gastroenterol. Hepatol. Bed Bench* **2017**, *10*, 131–136.
29. Tang, F.; Zhang, P.; Zhang, Q.; Xue, F.; Ren, J.; Sun, J.; Qu, Z.; Zhuge, X.; Li, D.; Wang, J.; et al. Isolation and characterization of a broad-spectrum phage of multiple drug resistant *Salmonella* and its therapeutic utility in mice. *Microb. Pathog.* **2019**, *126*, 193–198. [[CrossRef](#)]
30. Dallal, M.M.S.; Nikkhahi, F.; Alimohammadi, M.; Douraghi, M.; Rajabi, Z.; Foroushani, A.R.; Azimi, A.; Fardsanei, F. Phage therapy as an approach to control *Salmonella enterica* serotype Enteritidis infection in mice. *Rev. Soc. Bras. Med. Trop.* **2019**, *52*, 20190290. [[CrossRef](#)]
31. Bao, H.; Zhou, Y.; Shahin, K.; Zhang, H.; Cao, F.; Pang, M.; Zhang, X.; Zhu, S.; Olaniran, A.; Schmidt, S.; et al. The complete genome of lytic *Salmonella* phage vB\_SenM-PA13076 and therapeutic potency in the treatment of lethal *Salmonella* Enteritidis infections in mice. *Microbiol. Res.* **2020**, *237*, 126471. [[CrossRef](#)] [[PubMed](#)]
32. Seo, B.J.; Song, E.T.; Lee, K.; Kim, J.W.; Jeong, C.G.; Moon, S.H.; Son, J.S.; Kang, S.H.; Cho, H.S.; Jung, B.Y.; et al. Evaluation of the broad-spectrum lytic capability of bacteriophage cocktails against various *Salmonella* serovars and their effects on weaned pigs infected with *Salmonella* Typhimurium. *J. Vet. Med. Sci.* **2018**, *80*, 851–860. [[CrossRef](#)] [[PubMed](#)]
33. Jamal, M.; Bukhari, S.M.; Andleeb, S.; Ali, M.; Raza, S.; Nawaz, M.A.; Hussain, T.; Rahman, S.U.; Shah, S.S.A. Bacteriophages: An overview of the control strategies against multiple bacterial infections in different fields. *J. Basic Microbiol.* **2019**, *59*, 123–133. [[CrossRef](#)] [[PubMed](#)]

34. Jurczak-Kurek, A.; Gašior, T.; Nejman-Faleńczyk, B.; Bloch, S.; Dydecka, A.; Topka, G.; Necel, A.; Jakubowska-Deredas, M.; Narajczyk, M.; Richert, M.; et al. Biodiversity of bacteriophages: Morphological and biological properties of a large group of phages isolated from urban sewage. *Sci. Rep.* **2016**, *6*, 34338. [[CrossRef](#)] [[PubMed](#)]
35. Weber-Dabrowska, B.; Jończyk-Matysiak, E.; Zaczek, M.; Łobocka, M.; Łusiak-Szelachowska, M.; Górski, A. Bacteriophage procurement for therapeutic purposes. *Front. Microbiol.* **2016**, *7*, 1177. [[CrossRef](#)] [[PubMed](#)]
36. Sambrook, J.F.; Russell, D.W. *Molecular Cloning: A Laboratory Manual*, 3rd ed.; Cold Spring Harbor: New York, NY, USA, 2001; Volume 1.
37. Affolter, M.; Parent-Vaugois, C.; Anderson, A. Curing and induction of the Fels 1 and Fels 2 prophages in the Ames mutagen tester strains of *Salmonella typhimurium*. *Mutat. Res.* **1983**, *110*, 243–262. [[CrossRef](#)]
38. Figueroa-Bossi, N.; Bossi, L. Inducible prophages contribute to *Salmonella* virulence in mice. *Mol. Microbiol.* **1999**, *33*, 167–176. [[CrossRef](#)]
39. Garcia-Russell, N.; Elrod, B.; Dominguez, K. Stress-induced prophage DNA replication in *Salmonella enterica* serovar Typhimurium. *Infect. Genet. Evol.* **2009**, *9*, 889–895. [[CrossRef](#)]
40. Topka, G.; Bloch, S.; Nejman-Falenczyk, B.; Gašior, T.; Jurczak-Kurek, A.; Necel, A.; Dydecka, A.; Richert, M.; Węgrzyn, G.; Węgrzyn, A.; et al. Characterization of bacteriophage VB-EcoS-95, isolated from urban sewage and revealing extremely rapid lytic development. *Front. Microbiol.* **2019**, *9*, 3326. [[CrossRef](#)]
41. Caldeira, C.; Peabody, D.S. Stability and assembly in vitro of bacteriophage PP7 virus-like particles. *J. Nanobiotechnol.* **2007**, *5*, 10. [[CrossRef](#)]
42. Seemann, T. Prokka: Rapid prokaryotic genome annotation. *Bioinformatics* **2014**, *30*, 2068–2069. [[CrossRef](#)] [[PubMed](#)]
43. Marchler-Bauer, A.; Lu, S.; Anderson, J.B.; Chitsaz, F.; Derbyshire, M.K.; DeWeese-Scott, C.; Fong, J.H.; Geer, L.Y.; Geer, R.C.; Gonzales, N.R.; et al. CDD: A conserved Domain database for the functional annotation of proteins. *Nucleic Acids Res.* **2011**, *39*, D225–D229. [[CrossRef](#)]
44. Finn, R.D.; Clements, J.; Eddy, S.R. HMMER web server: Interactive sequence similarity searching. *Nucleic Acids Res.* **2011**, *39*, W29–W37. [[CrossRef](#)] [[PubMed](#)]
45. Naville, M.; Ghuillot-Gaudeffroy, A.; Marchais, A.; Gautheret, D. ARNold: A web tool for the prediction of Rho-independent transcription terminators. *RNA Biol.* **2011**, *8*, 11–13. [[CrossRef](#)] [[PubMed](#)]
46. McNair, K.; Bailey, B.A.; Edwards, R.A. PHACTS, a computational approach to classifying the lifestyle of phages. *Bioinformatics* **2012**, *28*, 614–618. [[CrossRef](#)]
47. Garneau, J.R.; Depardieu, F.; Fortier, L.C.; Bikard, D.; Monot, M. PhageTerm: A tool for fast and accurate determination of phage termini and packaging mechanism using next-generation sequencing data. *Sci. Rep.* **2017**, *7*, 8292. [[CrossRef](#)]
48. Stothard, P.; Wishart, D.S. Circular genome visualization and exploration using CGView. *Bioinformatics* **2005**, *21*, 537–539. [[CrossRef](#)]
49. Gautier, N.; Gouy, M.; Gautier, C. SeaView and Phylo\_win, two graphic tools for sequence alignment and molecular phylogeny. *Comput. Appl. Biosci.* **1996**, *12*, 543–548. [[CrossRef](#)]
50. Darling, A.C.E.; Mau, B.; Blattner, F.R.; Perna, N.T. Mauve: Multiple alignment of conserved genomic sequence with rearrangements. *Genome Res.* **2004**, *14*, 1394–1403. [[CrossRef](#)]
51. Swofford, D.L. *Phylogenetic Analysis Using Parsimony (and Other Methods)*, Version 4; Sinauer Associates: Sunderland, MA, USA, 2003.
52. Yoshida, R.; Nei, M. Efficiencies of the NJp, maximum likelihood, and Bayesian methods of phylogenetic construction for compositional and noncompositional genes. *Mol. Biol. Evol.* **2016**, *33*, 1618–1624. [[CrossRef](#)]

**Publisher's Note:** MDPI stays neutral with regard to jurisdictional claims in published maps and institutional affiliations.



© 2020 by the authors. Licensee MDPI, Basel, Switzerland. This article is an open access article distributed under the terms and conditions of the Creative Commons Attribution (CC BY) license (<http://creativecommons.org/licenses/by/4.0/>).